Interaction of Bragg solitons in fiber gratings

N. M. Litchinitser

The Institute of Optics and Rochester Theory Center of Optical Science and Engineering, University of Rochester, Rochester, New York 14627

B. J. Eggleton

Bell Laboratories, Lucent Technologies, Murray Hill, New Jersey 07974

C. M. de Sterke

School of Physics, University of Sydney, NSW 2006, Australia and Australian Photonics Cooperative Research Centre, Australian Technology Park, Eveleigh 1430, Australia

A. B. Aceves

Department of Mathematics and Statistics, University of New Mexico, Albuquerque, New Mexico 87131-1141

Govind P. Agrawal

The Institute of Optics and Rochester Theory Center of Optical Science and Engineering, University of Rochester, Rochester, New York 14627

Received May 22, 1998; revised manuscript received August 31, 1998

We investigate numerically the interaction between two copropagating Bragg solitons in a fiber grating. We find that, in the low-intensity limit, the interaction is reminiscent of the nonlinear Schrödinger solitons in that Bragg solitons attract or repel each other, depending on their relative phases. However, the relative phase between two Bragg solitons is found to depend on their initial separation. We discuss the implications of the numerical results for laboratory experiments. © 1999 Optical Society of America [S0740-3224(99)01301-6]

OCIS codes: 060.0060, 060.2310, 190.4370, 190.5530, 350.2770.

1. INTRODUCTION

Perhaps the most fascinating feature of solitons is their particle like behavior. Solitons tend to survive not only perturbations but also collisions with other solitons. In fact, solitons are guaranteed to survive collisions if they satisfy an integrable nonlinear equation such as the nonlinear Schrödinger equation (NLSE). Survival of two such colliding solitons is even more remarkable if one notes that solitons interact strongly with each other during the collision. For copropagating NLSE solitons, the interaction is either attractive or repulsive, depending on the relative phase between two solitons. In both cases the evolution of the NLSE soliton pair is well understood.[1–4]

The existence of solitons in one-dimensional nonlinear periodic media, such as fiber Bragg gratings, has been established theoretically for more than 10 years[5–9] and has also been confirmed experimentally.[10–15] Such Bragg solitons result from the balancing of the strong grating-induced dispersion with the Kerr nonlinearity of the fiber. Bragg solitons can propagate through the grating at any speed between zero and the speed of light inside optical fiber; propagation of Bragg solitons at 50–75% of the speed of light has been demonstrated experimentally.[10] However, Bragg solitons differ fundamentally from the NLSE solitons, since they are solutions of the nonlinear coupled-mode equations, which are nonintegrable. These solutions, which were first reported in their most general form by Aceves and Wabnitz,[8] are solitary waves, not true solitons. In general, survival during mutual interaction is not guaranteed for solitary waves. Collisions between two counterpropagating Bragg solitons having their central frequencies in the middle of the photonic bandgap were studied numerically by Aceves and Wabnitz.[8] Their results revealed that Bragg solitons tend to survive collisions, though their amplitudes and velocities are not necessarily preserved. Recently it was shown in Refs. 16 and 17 that Bragg solitons are well described by the NLSE at low intensities ($\sim$10 GW/cm^2). One may expect that, under such conditions, the interaction of Bragg solitons should reflect many of the features of NLSE solitons. It is noteworthy that Bragg solitons that have been demonstrated in the experiments[10–14] are within this low-intensity regime. Preliminary experimental results on Bragg soliton interaction in this regime have been reported recently.[18]

In this paper we extend the initial numerical results obtained by Aceves and Wabnitz[8] and study the interaction of Bragg solitons whose input central frequency lies just outside the stop band, a situation that corresponds closely to the recent experiments of Eggleton and colleagues.[10–14] We show that, in the low-intensity limit, Bragg soliton interaction exhibits features reminiscent of the NLSE solitons, except for the fact that their relative phase depends on the initial mutual separation. We study through numerical simulations the interaction between two copropagating Bragg solitons in both finite geometry, which corresponds to the laboratory experiments, and infinite geometry. In the finite geometry the coupling of light into the grating can complicate the interaction, whereas the coupling process can be ignored in an infinitely long grating. We also discuss the implication of our numerical results for observing the interaction of Bragg solitons experimentally.

2. INFINITE GRATING

We first consider the propagation of two copropagating Bragg solitons in an infinitely long grating, as shown in Fig. 1(a). In this case we can ignore the coupling issue at the interface between the uniform and the nonlinear periodic media. Following Ref. 19, we write the total optical field inside the grating as the sum of two counterpropagating waves:

$$E(z,t) = [E_+(z,t)\exp(ik_B z) + E_-(z,t) \times \exp(-ik_B z)]\exp(-i\omega_B t), \tag{1}$$

where the slowly varying amplitudes E_+ and E_- satisfy the following set of two nonlinear coupled-mode equations[9]:

$$i\frac{\partial E_+}{\partial z} + i\frac{n}{c}\frac{\partial E_+}{\partial t} + \kappa E_- + \Gamma_S|E_+|^2E_+ + 2\Gamma_\times|E_-|^2E_+ = 0, \tag{2}$$

$$-i\frac{\partial E_-}{\partial z} + i\frac{n}{c}\frac{\partial E_-}{\partial t} + \kappa E_+ + \Gamma_S|E_-|^2E_- + 2\Gamma_\times|E_+|^2E_- = 0. \tag{3}$$

Here ω_B is the Bragg frequency, k_B is the corresponding wave number, n is the average refractive index, c is the speed of light in vacuum, $\kappa = \pi\Delta n/\lambda_B$ is the coupling coefficient associated with the grating, and Γ_S and $\Gamma_\times$ are self- and cross-phase-modulation parameters, respectively.

A solution of these equations, corresponding to a two-parameter family of Bragg solitons, was found in Ref. 8. It can be written as

$$E_\pm = \alpha\tilde{E}_\pm \exp[i\eta(\theta)], \tag{4}$$

where

$$\tilde{E}_+ = \sqrt{\frac{\kappa}{2\Gamma_\times}}\left(\frac{1+\nu}{1-\nu}\right)^{1/4}\sin\delta\exp(i\sigma)\operatorname{sech}\left(\theta - i\frac{\delta}{2}\right),$$

$$\tilde{E}_- = -\sqrt{\frac{\kappa}{2\Gamma_\times}}\left(\frac{1-\nu}{1+\nu}\right)^{1/4}\sin\delta\exp(i\sigma)\operatorname{sech}\left(\theta + i\frac{\delta}{2}\right), \tag{5}$$

with $\theta = \kappa\gamma(\sin\delta)(z - \nu Vt)$, $\sigma = \kappa\gamma(\cos\delta)(\nu z - Vt)$, $\gamma = (1-\nu^2)^{-1/2}$, $V = c/n$, and

$$\frac{1}{\alpha^2} = 1 + \frac{\Gamma_S}{2\Gamma_\times}\frac{1+\nu^2}{1-\nu^2},$$

$$\exp[i\eta(\theta)] = \left[-\frac{\exp(2\theta)+\exp(-i\delta)}{\exp(2\theta)+\exp(i\delta)}\right]^{\frac{2\Gamma_S\nu}{2\Gamma_\times(1-\nu^2)+\Gamma_S(1+\nu^2)}}. \tag{6}$$

In Eqs. (5) and (6) the parameter ν can have any value in the range $|\nu| < 1$ and determines the soliton velocity. The parameter δ is also a free parameter and can have any value in the range $0 \leqslant \delta \leqslant \pi$. It determines the soliton amplitude and width. The parameter space (δ, ν) can be divided into two regions, as shown in Fig. 2, by use of the approximate condition $|\nu| < \sin\delta$ (Ref. 9), which determines approximately the range of parameters δ and ν for which the Bragg soliton has its central frequency inside the stop band (shaded area). The unshaded area represents Bragg solitons whose central frequency lies outside the stop band. In this paper we focus on the soliton propagation in the unshaded area.

For our numerical example, we choose the parameter values that correspond closely to the recent experiments[10–14] and take $\kappa = 10\ \mathrm{cm}^{-1}$, $\nu = 0.745$, and $\delta = 0.13$ (represented by a filled point in Fig. 2), which correspond to the full width at half-maximum (FWHM) soliton width $T_{\mathrm{FWHM}} = 1.763/(\kappa\gamma\nu V\sin\delta) = 60$ ps. To

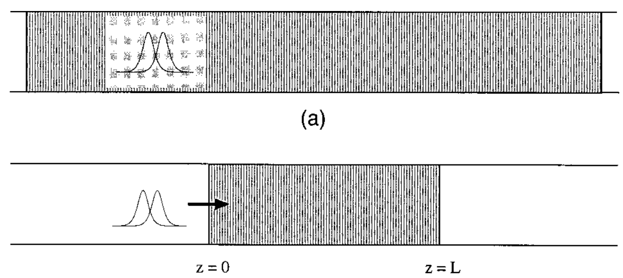

Fig. 1. Schematic of Bragg soliton interaction in (a) an infinitely long grating and in (b) a finite grating.

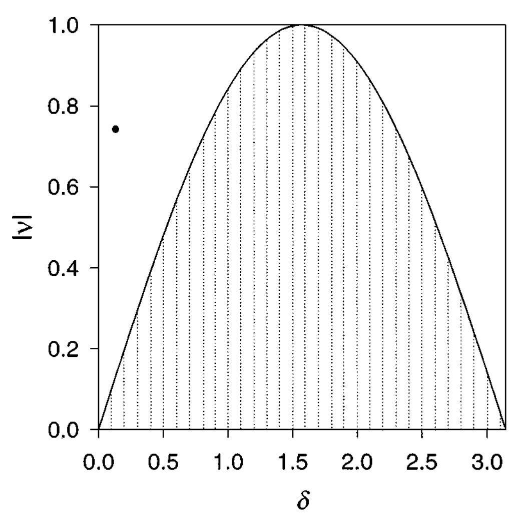

Fig. 2. Illustration of the grating stop band in the parameter space (δ, ν), showing the region for which the soliton central frequency lies inside the stop band (shaded area). The filled point represents the parameters used in numerical simulations.

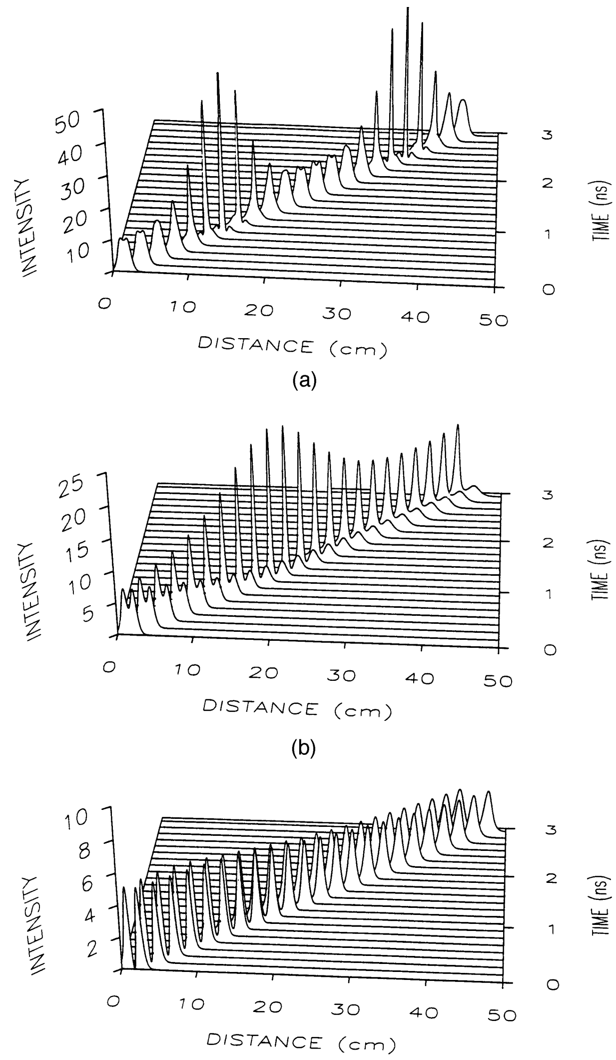

Fig. 3. Interaction of two Bragg solitons in an infinite fiber grating for three different values of their initial separation L_S: (a) $L_S = 1.113$ cm, (b) $L_S = 1.252$ cm, and (c) $L_S = 1.391$ cm. Other parameter values used are $\nu = 0.745$, $\delta = 0.13$, and $\kappa = 10\ \mathrm{cm}^{-1}$.

study interaction between two copropagating Bragg solitons, we solve Eqs. (2) and (3) numerically with the initial conditions

$$E_{\pm}(z, 0) = E_{\pm}(z - z_0, 0) + E_{\pm}(z - z_0 - L_S, 0), \quad (7)$$

where $E_{\pm}$ on the right-hand side are obtained from Eq. (4) and z_0 and $z_0 + L_S$ are the initial positions of the two solitons inside the infinite Bragg grating. We use a fourth-order collocation technique[20] to solve Eqs. (2) and (3). Results of our numerical simulation are shown in Fig. 3 for three different initial pulse separations: $L_S = 1.113$ cm [Fig. 3(a)], $L_S = 1.252$ cm [Fig. 3(b)], and $L_S = 1.391$ cm [Fig. 3(c)]. We discuss below how the initial separation L_S was chosen. Figure 3 shows that, for slightly different values of L_S, the interaction behavior is quite different even though we did not introduce any additional relative phase shift between the two solitons.

To understand the results shown in Fig. 3, we note that the solution to a linearized set of the coupled-mode equations [$\Gamma_S = \Gamma_{\times} = 0$ in Eqs. (2) and (3)] can be written in terms of two Bloch functions at the stop-band edges, each multiplied by a plane wave of the form $\exp[i(Qz - \Omega_{\pm}t)]$, where $\Omega_{\pm} = \pm V(Q^2 + \kappa^2)^{1/2}$. The solution of the nonlinear coupled-mode equations can also be written in terms of the same Bloch functions, but with a nonconstant amplitude.[21] To lowest order in the intensity, with the notation of Refs. 9 and 21, the coupled-mode equations have the solution

$$\begin{bmatrix} E_+ \\ E_- \end{bmatrix} = a(z, t)\begin{bmatrix} A_+ \\ A_- \end{bmatrix}\exp[i(Qz - \Omega_{\pm}t)]. \quad (8)$$

If we assume that the amplitude $a(z, t)$ varies on a much slower scale than that associated with the plane wave and make use of the slowly varying envelope approximation, we find that the amplitude $a(z, t)$ satisfies the NLSE.[16]

In the notation of Eq. (8), Eq. (7) can be written in the form

$$\begin{aligned}\begin{bmatrix} E_+(z, 0) \\ E_-(z, 0) \end{bmatrix} &= a(z - z_0, 0)\begin{bmatrix} A_+ \\ A_- \end{bmatrix}\exp[iQ(z - z_0)] \\ &\quad + a[z - (z_0 + L_S), 0]\begin{bmatrix} A_+ \\ A_- \end{bmatrix} \\ &\quad \times \exp[iQ(z - z_0)]\exp(-iQL_S). \quad (9)\end{aligned}$$

From Eq. (9) we can see that two solitons spaced by L_S exhibit a relative phase difference QL_S when the field envelopes $E_{\pm}$ are considered. Therefore, to study the interaction of truly in-phase solitons, the separation L_S must be chosen such that $QL_S = 2\pi m$, where m is an integer. In other words, if the soliton separation is L_S, then a phase difference of ϕ between the slowly varying amplitudes $a(z, t)$ associated with the two Bragg solitons corresponds to a phase difference of $\phi - QL_S$ between the field envelopes $E_{\pm}(z_0)$ and $E_{\pm}(z_0 + L_S)$. Hence, to consider a pair of truly in-phase solitons, we must choose

$$\phi = QL_S. \quad (10)$$

Of course, the choice of L_S is also dictated by the soliton width, since L_S should be large enough to resolve one soliton from another yet small enough to let their tails overlap.[1] To be more accurate, we should include the z-dependent part of the phase of $a(z, t)$ in determining L_S. We can obtain this phase by following Ref. 16.

The values of L_S in Fig. 3 were chosen such that Fig. 3(a) corresponds to in-phase solitons; Fig. 3(b), to a phase shift of $\pi/2$; and Fig. 3(c), to out-of-phase solitons. As can be seen in Fig. 3, in-phase solitons attract each other [Fig. 3(a)], while out-of-phase solitons repel each other [Fig. 3(c)]. In the case of the $\pi/2$ phase shift, energy flows from one soliton to another [Fig. 3(b)]. Note also that in Fig. 3(a) two solitons collapse and recover periodically as they propagate through the grating, similar to the case of NLSE solitons.[2,3]

In summary, we found that in the low-intensity limit the interaction is reminiscent of nonlinear Schrödinger solitons in that Bragg solitons attract or repel, depending on their relative phases, but that their relative phase depends on the initial mutual separation.

3. FINITE GRATING

Because one of the aims of a numerical analysis is to model laboratory experiments, we now consider the propagation of two Bragg solitons in a uniform finite grating of length L [Fig. 1(b)]. While pulses can be characterized experimentally only outside the grating, numerical simulations also show how the soliton pair evolves inside the grating—information crucial for understanding the interaction process. Numerical modeling also allows us to study the soliton interaction in long gratings, which are not readily available for experiments. As above, we solve the nonlinear coupled-mode equations (2) and (3) numerically but use the boundary conditions appropriate for a finite grating. More specifically, the coupling of light from a uniform medium to a nonlinear fiber grating must be considered. Assuming that two sech-shaped pulses, delayed by a time interval T_S, are incident upon the left-hand boundary at $z = 0$, the boundary conditions become

$$E_+(0, t) = A_0 \operatorname{sech}[(t - T_S)/T_0] + A_0 \operatorname{sech}(t/T_0)\exp(i\phi), \qquad (11)$$

$$E_-(L, t) = 0, \qquad (12)$$

where $T_0 = T_{\mathrm{FWHM}}/1.763$ and ϕ is the relative phase shift between the two incident pulses. The initial condition is now taken to be $E_\pm(z, 0) = 0$.

The amplitude A_0 in Eq. (9) has been chosen, according to the procedure described in Ref. 9, such that a pair of Bragg solitons is formed close to the front end of the grating. Briefly, knowing the optical field associated with the Bragg soliton [Eqs. (5)] and the transmission coefficient of the grating, one can find the external field required for exciting the Bragg soliton with a fixed set of values for the parameters δ and ν. To demonstrate the effectiveness of this coupling procedure, we first consider the case of a single pulse launched into the fiber grating. We show in Fig. 4 the evolution of an input pulse launched with three different initial amplitudes A_0. Figure 4(a) corresponds to the regime for which the input field is too weak to form a Bragg soliton. Figure 4(b) corresponds to the case in which the input field is chosen through the procedure described in Ref. 9. A Bragg soliton is formed close to the front end of the grating and propagates undistorted along the length of the grating. In the case in which the input field is stronger than that necessary to form the Bragg soliton, the pulse sheds radiation as it propagates along the grating, as shown in Fig. 4(c).

We now consider the interaction of Bragg solitons excited by launching two input pulses separated by a time interval T_S by using Eqs. (11) and (12). We also take $\phi = 0$ in Eq. (11), which implies no relative phase shift between the two input pulses. To facilitate the comparison between finite and infinite gratings, numerical simulations were performed by use of the same values for T_S (corresponding to $L_S = \nu V T_S$), as in Section 2. Figure 5 shows that the results for a finite grating are quite different from those obtained for an infinite grating (Fig. 3). For a finite grating the interaction is attractive for any initial time delay T_S (with $\phi = 0$), while for an infinite grating it can be attractive or repulsive, depending on the

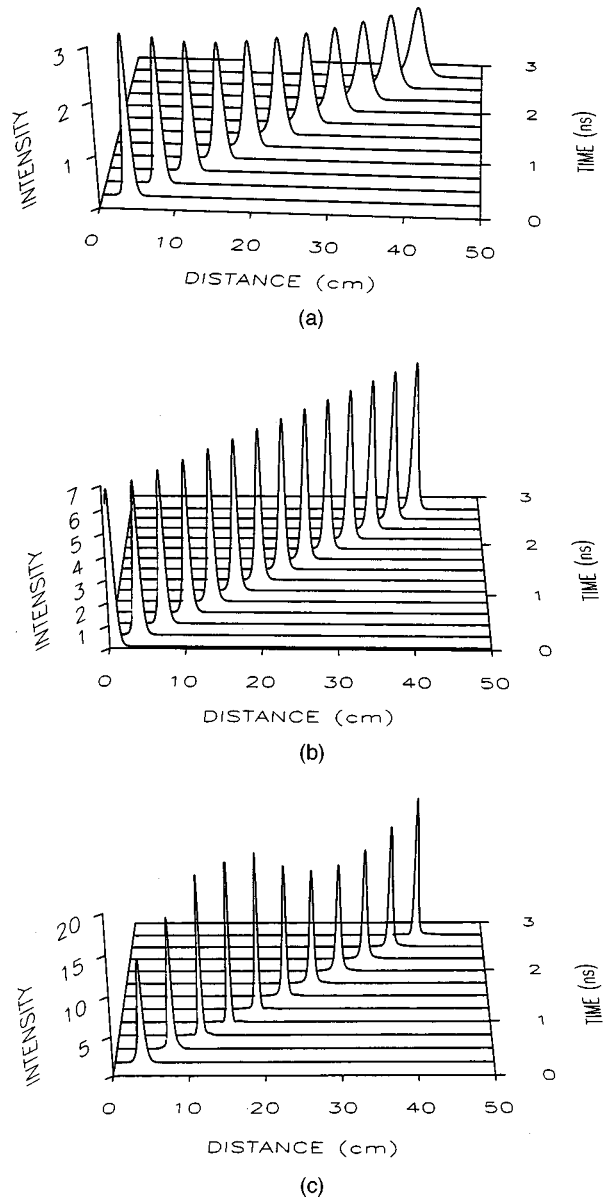

Fig. 4. Evolution of a 60-ps sech-shaped pulse in a 50-cm-long fiber grating for an input pulse intensity of (a) $I_0 = A_0{}^2 = 3\ \mathrm{GW/cm^2}$, (b) $I_0 = 5.94\ \mathrm{GW/cm^2}$, and (c) $I_0 = 10\ \mathrm{GW/cm^2}$. A Bragg soliton is formed only in case (b).

initial pulse separation. This apparent discrepancy between finite and infinite gratings can be understood from Eq. (8), which shows that the phase accumulated on propagation over a distance z is Qz. Thus two in-phase solitons outside the grating are always in phase inside the grating as well, as the extra propagation of the first soliton over the distance L_S inside the grating provides precisely the phase required for two solitons to be in phase in an infinite grating [see Eq. (10)]. If we now change the initial phase shift from $\phi = 0$ to $\phi = -QL_S$ and perform the simulations with the modified boundary condition

$$E_+(0, t) = A_0 \operatorname{sech}[(t - T_S)/T_0] + A_0 \operatorname{sech}(t/T_0)\exp(-iQL_S), \qquad (13)$$

we obtain the results shown in Fig. 6. A comparison of Figs. 3 and 6 shows that the interaction features for a finite grating are now almost identical to those obtained in Section 2 for an infinite grating (see Fig. 3). We notice that for the smallest pulse separation [Fig. 6(a)] the interaction features are slightly different from those shown in Fig. 3(a). This difference may be attributed to the nonlinear nature of soliton interaction: Formation of the first Bragg soliton changes the grating enough that it affects formation of the second soliton. This effect becomes more severe for smaller pulse separations and may complicate launching of a soliton pair. As the initial pulse separation increases, this effect should diminish, as can also be seen in Fig. 6. It is noteworthy that one can reverse the direction of energy flow in Fig. 6(b) simply by changing the sign of the relative phase shift. Similar behavior has been observed for two fundamental spatial solitons.[4]

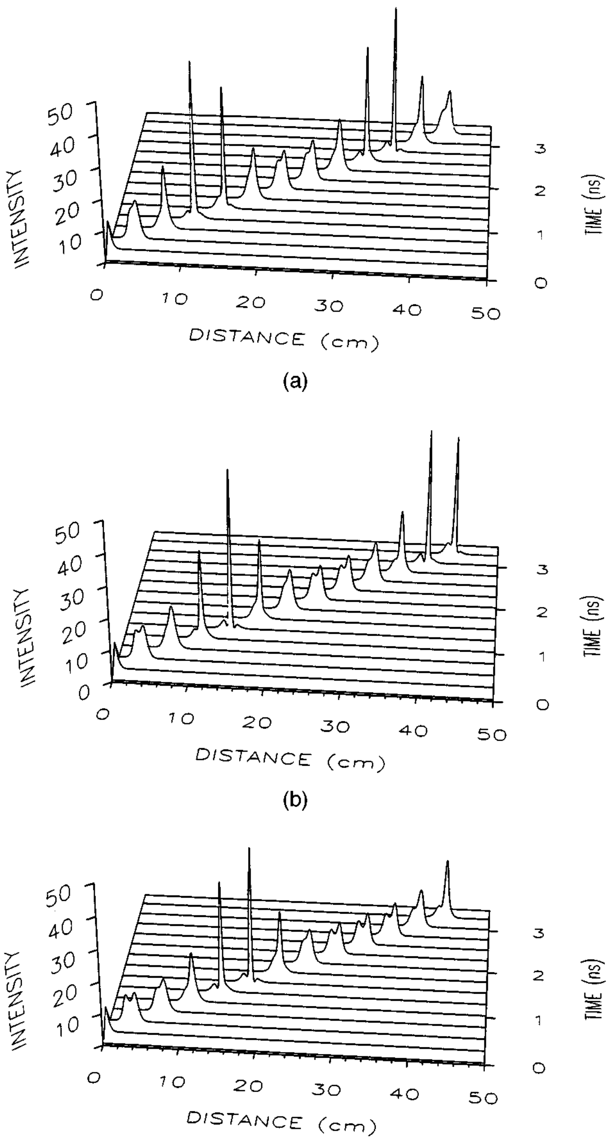

Fig. 5. Interaction of two Bragg solitons in a 50-cm-long fiber grating for the same initial soliton separations as in Fig. 3. The input pulses have a width of $T_{\mathrm{FWHM}} = 60$ ps and a peak intensity $I_0 = 5.94$ GW/cm^2.

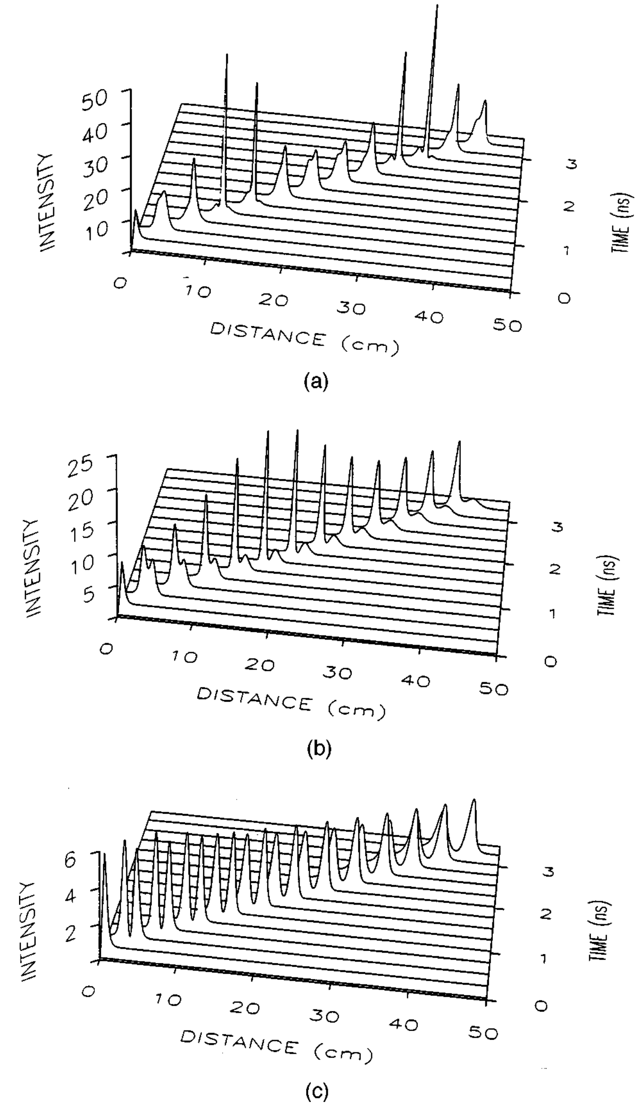

Fig. 6. Interaction of two Bragg solitons in a 50-cm-long fiber grating for the same parameters as in Fig. 5, but with three different relative phase shifts: (a) $\phi = 0$, (b) $\phi = \pi/2$, and (c) $\phi = \pi$.

4. EXPERIMENTAL CONSIDERATIONS

We now discuss the implications of the numerical results obtained in Section 3 for designing realistic laboratory experiments, where grating lengths of 10 cm or less are typically used. In the previous sections we found that the in-phase interaction leads to a periodic collapse and revival of two Bragg solitons. To observe this behavior in an experiment, the collapse distance L_c should be less than the grating length L.

In the limit of low-intensity solitons considered in this paper, Bragg solitons are well described by the NLSE,[16] and therefore the results obtained for the NLSE solitons can be used for Bragg solitons as well. For NLSE solitons, the dependence of soliton separation on the propagation distance and on the initial soliton separation T_S has been studied analytically by use of the inverse scattering technique,[1,22,23] resulting in the following expression for the collapse distance:

$$L_c = \frac{\pi \sinh(T_S/T_0)\cosh(T_S/2T_0)}{T_S/T_0 + \sinh(T_S/T_0)} \frac{T_0^2}{|\beta_2|}, \tag{14}$$

where β_2 is the effective group-velocity dispersion introduced by the grating given by[24,25]

$$\beta_2 = -\frac{1}{V^2} \frac{\kappa^2}{[(\Omega/V)^2 - \kappa^2]^{3/2}}. \tag{15}$$

For our numerical examples considered in Sections 2 and 3 [Figs. 3(a) and 6(a)], we find from Eq. (14) that $L_c \approx 23$ cm, which is in good agreement with the results shown in Figs. 3(a) and 6(a). Soliton interaction can be observed in experiment if the grating length $L > L_c$. Therefore, to observe soliton collapse in a 10-cm-long grating, one should decrease the collapse distance either by using shorter pulses or by increasing β_2. The use of shorter pulses is not practical because of their relatively wide spectrum, which makes operation near the edge of the photonic bandgap hard to realize. Moreover, higher input pulse intensities necessary to form shorter solitons can lead to significant damage of the grating. Equation (15) shows that β_2 increases close to an edge of the photonic bandgap, i.e., when $\Omega/V \rightarrow \kappa$, which corresponds to slowly moving solitons. For example, from Eq. (14), $L_c \approx 9$ cm when $\Omega/V = 12.5\ \mathrm{cm}^{-1}$ and $\kappa = 10\ \mathrm{cm}^{-1}$. Thus the experimental observation of the collapse of two Bragg solitons would require either low-velocity solitons or a relatively long grating.

5. CONCLUSIONS

We have studied numerically the interaction between two copropagating Bragg solitons in a fiber grating. Our results reveal that, in the low-intensity limit, Bragg solitons can attract or repel each other or can exchange energy, depending on their initial separation. Bragg soliton interaction exhibits features reminiscent of the NLSE solitons except for the new feature that the relative phase of two Bragg solitons depends on their initial separation. Finally, we discussed the implications of our numerical results for observing the interaction of Bragg solitons experimentally. In the future we hope to address in detail the interaction of Bragg solitons in the nonintegrable limit.

ACKNOWLEDGMENTS

We thank T. G. Brown and A. V. Buryak for fruitful discussions. N. M. Litchinitser thanks the Aileen S. Andrew Foundation for a postdoctoral fellowship. This research is partially supported by the National Science Foundation under grant PHY 94-15583 and by the Australian Research Council.

REFERENCES

1. J. P. Gordon, “Interaction forces among solitons in optical fibers,” Opt. Lett. **8**, 596–598 (1983).
2. F. M. Mitschke and L. F. Mollenauer, “Experimental observation of interaction forces between solitons in optical fibers,” Opt. Lett. **12**, 407–409 (1987).
3. J. S. Aitchison, A. M. Weiner, Y. Silberberg, D. E. Leaird, M. K. Oliver, J. L. Jackel, and P. W. E. Smith, “Experimental observation of spatial soliton interactions,” Opt. Lett. **16**, 15–17 (1991).
4. M. Shalaby, F. Reynaud, and A. Barthelemy, “Experimental observation of spatial soliton interactions with a $\pi/2$ relative phase difference,” Opt. Lett. **17**, 778–780 (1992).
5. W. Chen and D. L. Mills, “Gap solitons and nonlinear optical response of superlattices,” Phys. Rev. Lett. **58**, 160–163 (1987).
6. J. E. Sipe and H. G. Winful, “Nonlinear Schrödinger solitons in a periodic structure,” Opt. Lett. **13**, 132–133 (1988).
7. D. N. Christodoulides and R. I. Joseph, “Slow Bragg solitons in nonlinear periodic structures,” Phys. Rev. Lett. **62**, 1746–1749 (1989).
8. A. B. Aceves and S. Wabnitz, “Self-induced transparency solitons in nonlinear refractive periodic media,” Phys. Lett. A **141**, 37–42 (1989).
9. C. M. de Sterke and J. E. Sipe, “Gap solitons,” in *Progress in Optics*, E. Wolf, ed. (North-Holland, Amsterdam, 1994), Vol. 33, pp. 203–260.
10. B. J. Eggleton, R. E. Slusher, C. M. de Sterke, P. A. Krug, and J. E. Sipe, “Bragg grating solitons,” Phys. Rev. Lett. **76**, 1627–1630 (1996).
11. C. M. de Sterke, B. J. Eggleton, and P. A. Krug, “High-intensity pulse propagation in uniform gratings and grating superstructures,” J. Lightwave Technol. **15**, 1494–1502 (1997).
12. B. J. Eggleton, R. E. Slusher, T. A. Strasser, and C. M. de Sterke, “High intensity pulse propagation in fiber Bragg gratings,” in *Bragg Gratings, Photosensitivity, and Poling in Glass Fibers and Waveguides: Applications and Fundamentals*, Vol. 17 of 1997 OSA Technical Digest Series (Optical Society of America, Washington, D.C., 1997), paper BMB1-1.
13. B. J. Eggleton, C. M. de Sterke, and R. E. Slusher, “Nonlinear pulse propagation in Bragg gratings,” J. Opt. Soc. Am. B **14**, 2980–2993 (1997).
14. B. J. Eggleton, C. M. de Sterke, R. E. Slusher, A. Aceves, J. E. Sipe, and T. A. Strasser, “Modulational instabilities and tunable multiple soliton generation in apodized fiber gratings,” Opt. Commun. **149**, 267–271 (1998).
15. D. Taverner, N. G. R. Broderick, D. T. Richardson, R. I. Laming, and M. Ibsen, “Nonlinear self-switching and multiple gap-soliton formation in a fiber Bragg grating,” Opt. Lett. **23**, 328–330 (1998).
16. C. M. de Sterke and B. J. Eggleton, “Bragg solitons and the nonlinear Schrödinger equation,” Phys. Rev. E (to be published).
17. T. Iizuka and M. Wadati, “Grating solitons in optical fibers,” J. Phys. Soc. Jpn. **66**, 2308–2313 (1997).
18. B. J. Eggleton, R. E. Slusher, N. M. Litchinitser, G. P. Agrawal, and C. M. de Sterke, “Experimental observation of interaction of Bragg solitons,” in *International Quantum Electronics Conference (IQEC)*, Vol. 7 of 1998 OSA Technical Digest Series (Optical Society of America, Washington, D.C., 1998), paper QTuJ5.
19. H. G. Winful, “Pulse compression in optical fiber filters,” Appl. Phys. Lett. **46**, 527–529 (1985).
20. C. M. de Sterke, K. R. Jackson, and B. D. Robert, “Nonlinear coupled mode equations on a finite interval: a numerical procedure,” J. Opt. Soc. Am. B **8**, 403–412 (1991).
21. C. M. de Sterke, N. G. R. Broderick, B. J. Eggleton, and M. J. Steel, “Nonlinear optics in fiber gratings,” Opt. Fiber Technol. **2**, 253–268 (1996).
22. G. P. Agrawal, *Fiber-Optic Communication Systems*, 2nd ed. (Wiley, New York, 1997).
23. C. Desem and P. L. Chu, IEE Proc.-J: Optoelectron. **134**, 145–151 (1987).
24. P. St. J. Russell, “Bloch wave analysis of dispersion and pulse propagation in pure distributed feedback structures,” J. Mod. Opt. **38**, 1599–1619 (1991).
25. N. M. Litchinitser, B. J. Eggleton, and D. B. Patterson, “Fiber Bragg gratings for dispersion compensation in transmission: Theoretical model and design criterion for nearly ideal pulse compression,” J. Lightwave Technol. **15**, 1303–1313 (1997).